

Effect of Tadalafil on Apoptosis and Proliferation in Urinary Bladder Mucosa after Chemically Induced Hemorrhagic Cystitis; A Histological and Immunohistochemical Study

Shereen S. Elabd, Marwa A. A. Ibrahim and Mona T. Sadek

Department of Histology and Cell Biology, Faculty of Medicine, Tanta University, Egypt

ABSTRACT

Introduction: Haemorrhagic cystitis (HC) can be chemically induced by cyclophosphamide (CYP) injection; it is mainly used as an immunosuppressive and antineoplastic drug. Tadalafil (TAD) a phosphodiesterase type-5 inhibitor has vasodilator, anti-inflammatory and anti-apoptotic effects. It is mainly used for the treatment of erectile dysfunction and pulmonary arterial hypertension.

Aim of the Work: This work aimed to verify the effect of tadalafil on apoptosis and proliferation on the injured bladder mucosa after chemically induced HC.

Material and Methods: Thirty-six adult male albino rats were randomly divided into four groups; group I was the control group, group II was TAD-treated group, group III was CYP-treated group and group IV was TAD-CYP treated group. Groups III and IV were subdivided into two subgroups (a and b), subgroups IIIa and IVa were euthanized after one day while subgroups IIIb and IVb were euthanized after 10 days. Urinary bladder specimens were processed for light and electron microscopic examination and immunohistochemical analysis of caspase-3 and Ki-67.

Results: Subgroup IIIa revealed haemorrhage and decrease of urothelium thickness with presence of denuded areas. Subgroup IIIb showed restoration of urothelium with focal denuded areas. Both subgroups showed a significant increase in apoptotic index while subgroup IIIb showed a significant increase in proliferative index. Subgroup IVa revealed a significant decrease in apoptosis associated with a significant increase in proliferation, thereby limiting cellular loss. Subgroup IVb; showed a significant decrease in both apoptosis and proliferation indicated prevention of the developed hyperplasia of the urothelium. By transmission electron microscopy, the terminal differentiation of superficial cells of group IV was expressed by presence of an angular contour.

Conclusion: TAD-CYP co-treatment provides a positive impact on the apoptosis, proliferation, and the histological changes of HC on urinary bladder mucosa. Therefore, further studies are required to elucidate the protective effect of TAD on CYP-induced HC.

Received: 09 December 2020, **Accepted:** 02 February 2021

Key Words: Caspase-3; cyclophosphamide; ki-67; tadalafil; urinary bladder.

Corresponding Author: Shereen S. Elabd, MD, Department of Histology and Cell Biology, Faculty of Medicine, Tanta University, Egypt, **Tel.:** +20 10062 69505, **E-mail:** shereen.elabd@med.tanta.edu.eg

ISSN: 1110-0559, Vol. 45, No.1

INTRODUCTION

Cyclophosphamide (CYP) is a nitrogen mustard alkylating agent. It is mainly used as an immunosuppressive and antineoplastic agent for the treatment of various cancers^[1,2]. It exerts its cytotoxic effect by alkylation of guanine group of DNA molecule making the double strands unable to uncoil and separate, thus preventing multiplication of cells and leading them to induce apoptosis. These agents do not discriminate between cycling and resting cells, so they are even more toxic for rapidly dividing cells^[3].

One of the most serious adverse effects of CYP is hemorrhagic cystitis (HC)^[4]. It is important to elucidate the mechanism of CYP-induced HC in order to minimize the toxic and dose-limiting side effects. CYP is converted by oxidative enzyme cytochrome P450 in the liver into active product acrolein that is freely filtered by the kidneys to accumulate in the bladder^[3]. Acrolein is the causative agent responsible for CYP-induced HC^[5]. It increases reactive

oxygen species (ROS) in the urothelium, thus inducing oxidative stress and depletion of antioxidant enzymes leading to neutrophil infiltration and necrosis^[6]. Some researchers demonstrated an increase in proinflammatory mediators as interleukin-1 β (IL- β), tumour necrosis factor- α (TNF α) after injection of CYP^[7]. Additionally, previous studies demonstrated apoptotic changes in the testis with the use of CYP^[8].

Elimination of the harmful secondary effects of CYP makes the treatment more comfortable and enables the patients to tolerate this cytotoxic drug. There have been many trials to impede CYP-induced cystitis with pre-treatment with different drugs; such as 2-mercaptoethane sulfonate (Mesna)^[9], selenium^[11], melatonin^[10], and pomegranate^[11]. These compounds have been shown to partially suppress the magnitude of CYP-induced cystitis. Some investigators combined antioxidants as selenium and anti-inflammatory drugs as simvastatin together with CYP hoping for the elimination

of its urotoxicity^[1,2]. Consequently, an antioxidant and anti-apoptotic agent might provide a good preventive choice to reduce the hazardous effects of CYP without distressing its immunomodulatory effects^[1].

Tadalafil, a phosphodiesterase type-5 (PDE5) inhibitor, was approved by the US Food and Drug Administration (FDA) for the treatment of erectile dysfunction and lower urinary tract symptoms secondary to benign prostatic hyperplasia^[12,13]. PDE5 inhibitors are known to increase the amount of cyclic guanosine monophosphate (cGMP) and nitric oxide (NO) in the endothelium and smooth muscle of the corpus cavernosum, the prostate, and the bladder^[14]. It was found that PDE5 is highly expressed in the lower urinary tract and its supporting vasculature. PDE5 inhibition potentially modulates bladder afferent nerve activity, decreases smooth muscle cell proliferation, and relaxes smooth muscle cells in the prostate, bladder neck, and their supporting vasculature leading to increase blood perfusion to the lower urinary tract^[15]. Moreover, several preceding studies reported the anti-inflammatory and anti-apoptotic effects of tadalafil^[16].

In rodents, a single dose of CYP injection causes severe destruction of the bladder urothelium by necrosis and apoptosis leaving few surviving cells^[17]. After a few days; the survived cells maintain their capacity to proliferate and re-epithelialize and the denuded areas are observed as reversible hyperplasia, just for rapid maintaining of physical urothelial barrier lacking the terminally differentiated umbrella cells. The hyperplastic urothelium returns to normal by decreasing its proliferative capacity by enhancing apoptosis^[18]. The urothelial regeneration is followed by terminal differentiation of the outermost urothelial cells. The extended damage done by CYP causes exposure of the undifferentiated apical cells with microvilli, which eventually turns into terminally differentiated superficial umbrella cells with rigid-looking microridges^[19].

Caspase-3; one of the effector or executioner caspases, breaks down numerous substrates, including cytokeratins, plasma membrane cytoskeletal proteins, nuclear proteins, and others, which eventually induce the morphological and biochemical changes seen in apoptotic cells^[20]. Ki-67 is a classic marker of cell proliferation and an important prognostic indicator of aggressiveness, progression, and recurrence of tumors. Ki-67 is a DNA-binding nuclear protein that is preferentially expressed through all phases of the cell cycle wherein it is absent from resting cells in G0 phase, thus it is an excellent biomarker that express cell proliferation^[21,22].

This work was carried out to verify the effect of tadalafil on apoptosis and proliferation in the injured urinary bladder mucosa after chemically induced haemorrhagic cystitis in adult male albino rats using different histological and immunohistochemical methods.

MATERIALS AND METHODS

Experimental design

Thirty-six adult male albino rats (weighing 100-150g each) were housed in the animal house of the Histology department of the Faculty of Medicine, Tanta University. They were kept in plastic cages under adequate ventilation, temperature (25±2oC), and a 12h/12h alternating light-dark cycle. Animals had free access to food and water ad libitum. The study was approved by the Research Ethics committee of the Faculty of Medicine, Tanta University (No. 34342/12/20).

The rats were equally divided into four main groups

Group I (the control group) (n=6): this group was subdivided into two subgroups; Subgroup Ia (n=2) was left without treatment, and subgroup Ib (n=4) was given 1 ml of distilled water through a gastric tube every day; to be subdivided equally into two subgroups; subgroup Ib1 was euthanized after one day while subgroup Ib2 was euthanized after 10 days.

Group II (Tadalafil-treated group) (n=6): This group was treated with tadalafil (TAD) (Cialis®; Eli Lilly and Co pharmaceutical company, Cambridge, MA, USA) at a dose of 10mg/kg once daily for 10 days^[23]. The crushed tadalafil tablets were dissolved in distilled water and orally administered through a gastric tube.

Group III (CYP-treated group) (n=12): Acute cystitis was chemically induced by a single intraperitoneal injection of cyclophosphamide (CYP) (Sigma-Aldrich co., St. Louis, Missouri, USA) at a dose of 100 mg/kg dissolved in distilled water^[10]. The animals were further subdivided into two equal subgroups; subgroup IIIa was euthanized after one day of the treatment, and subgroup IIIb was euthanized after ten days of the treatment.

Group IV (CYP-TAD-treated group) (n=12): This group was treated with both TAD and CYP in the same doses and duration as described in groups II and III respectively. The animals were further subdivided into two equal subgroups; subgroup IVa was euthanized after one day of the treatment, and subgroup IVb was euthanized after ten days of the treatment.

At the appropriate time, the rats were euthanized with pentobarbital (40 mg/kg)^[24] and the urinary bladders were rapidly dissected out. One half of the urinary bladder was processed for light microscopy, and the other half was processed for transmission electron microscopy.

Light microscopic study

Urinary bladder specimens were immediately fixed in 10% neutral buffered formalin, washed, dehydrated, cleared and embedded in paraffin. Sections of 5µm thickness were stained with hematoxylin and eosin (H&E)^[25].

Immunohistochemical staining for detection of Ki-67 and activated caspase-3

Immunohistochemical staining was performed using the streptavidin-biotin-peroxidase complex technique to detect activated caspase-3 and Ki-67 antigens. After deparaffinization and rehydration, antigen retrieval was done by boiling in sodium citrate buffer (10 mM, pH 6.0) for 10-20 min followed by cooling at room temperature for 20 min. The endogenous peroxidase activity was blocked by 3% hydrogen peroxide/methanol for 20 minutes followed by washing. The sections were incubated in 5% human serum albumin (blocking protein) for 30 minutes followed by washing three times in phosphate-buffered saline (PBS). The sections were then incubated overnight at 4°C with primary antibodies; anti-caspase-3 (PP229AA polyclonal antibody, obtained from Biocare Medical Company, USA) or anti-Ki67 (ab9260 polyclonal antibody, obtained from Sigma-Aldrich Company, Germany). The sections were further washed three times for 10 minutes each in PBS. The slides were incubated with biotinylated secondary antibody for 30 min at room temperature, then washed in PBS and incubated for one hour with ABC solution (peroxidase-labelled streptavidin). The reaction was visualized with 0.05% diaminobenzidine (DAB) and counterstained with hematoxylin before mounting^[26]. Positive results of activated caspase-3 appeared as cytoplasmic and/or nuclear reaction, and for Ki-67 appeared as diffuse nuclear brown stain. Positive control for Ki-67 was from the normal tonsil while for caspase-3 was from the placenta. Negative control was run automatically by omitting the primary antibody^[26].

Transmission Electron microscopic study

Small pieces (1 mm³) of the urinary bladder specimens were fixed in 2.5% buffered glutaraldehyde (pH 7.3) for 2h at 4°C. Specimens were postfixed in 1% osmium tetroxide (pH 7.3) and then were dehydrated in ascending grades of alcohol and then passed through two changes of propylene oxide and embedded in epoxy resin. Ultrathin sections (60 nm thick) were cut, mounted on copper grids, and stained with uranyl acetate and lead citrate^[27]. The grids were then examined and photographed with the transmission electron microscope JOEL (JEOL-JEM-100 transmission electron microscope (Tokyo, Japan) at the Electron Microscopic Unit, Faculty of Medicine, Tanta University.

Morphometric study

A Leica microscope (DM500, Switzerland) coupled to a Leica digital camera (ICC50, Switzerland) was used for image acquisition. The software "ImageJ" (version 1.48v National Institute of Health, Bethesda, Maryland, USA) was used for image analysis in Faculty of Medicine, Tanta University. Ten different non-overlapping randomly selected fields from each slide at a magnification of 400 were examined to quantitatively evaluate:

1. The mean urothelium thickness (µm)

2. Apoptosis index (number of caspase-3 immunopositive cells x 100 / the total number of urothelial cells)^[28,29].
3. Proliferation index (number of Ki-67 immunopositive cells x 100 / the total number of urothelial cells)^[28,29].

Statistical analysis

The data were analyzed by using one-way analysis of variance (ANOVA) followed by Tukey's test for comparison between the groups using statistical package for social sciences statistical analysis software (IBM SPSS Statistics for Windows, IBM Corp, Version 22.0. Armonk, NY, USA). Differences were regarded significant if the probability value $p < 0.05$ and highly significant if $p < 0.001$ ^[30].

RESULTS

During the study period no mortality was recorded in the experimental animals.

Light Microscopic findings

H&E staining

Groups (I&II)

H&E stained sections from both control subgroups and tadalafil-treated group similarly revealed the normal histological architecture of the urinary bladder with its highly folded lining mucosa composed of urothelium and lamina propria. The urothelium was formed of transitional epithelium consisting of three to five rows; the superficial layer was formed of dome-shaped cells with characteristic angular contour bulging into the lumen, followed immediately by numerous pear-shaped cells then finally a basal layer resting on the lamina propria. The lamina propria containing blood capillaries was subdivided into a superficial layer and a deep one. The muscular layer was subdivided into three interlaced layers of smooth muscle cells; thin inner and outer longitudinal layers and a thick middle circular layer (Figures 1,2).

Group (III)

H&E stained sections from subgroup IIIa (after 1 day of a single injection of CYP) revealed haemorrhage and extensive loss of urothelial cells. The urothelium showed a marked decrease in its thickness to be formed of one or two rows of cells. Focal ulcerated areas with detached cells leaving denuded areas of the underlying highly cellular lamina propria (Figure 3). Most cells coalesced with vacuolated cytoplasm and dark pyknotic nuclei. The deep lamina propria appeared less cellular with empty spaces enclosing congested blood capillaries (Figure 4).

Moreover, sections from subgroup IIIb (after 10 days of a single injection of CYP) showed restoration of the transitional epithelium lining the mucosal folds, which appeared formed of many layers, however, focal loss of urothelium leaving denuded areas of lamina propria in addition to sloughed tissues in the lumen were still detected in certain areas. Most of the urothelial cells were vacuolated

with dark pyknotic nuclei and wide intercellular spaces. The submucosa was disrupted with focal areas of massive mononuclear cells infiltration and dilated congested blood vessels (Figures 5,6).

Group (IV)

Histological examination of sections from subgroup IVa (after 1 day of receiving both CYP&TAD) showed an apparent decrease of the urothelium thickness compared to the control, yet, it was formed of two or more urothelial cells. However, there were few focal areas of separation and cell loss with no evident denuded areas. Some superficial cells appeared enlarged and vacuolated. The submucosa still showed neutrophils infiltration and dilated congested blood capillaries (Figure 7).

Nevertheless, examination of sections from subgroup IVb (after 10 days of receiving both CYP&TAD) revealed an almost full restoration of urothelium thickness with apparently normal cells, furthermore, the superficial dome cells were evident with their characteristic angular contour, yet, minimal separations between urothelial cells were still observed. The lamina propria appeared normal with no inflammatory cells nor congested dilated capillaries. (Figure 8).

Morphometrical analysis of the mean urothelium thickness (μm) of subgroups IIIa and IVa (5.94 ± 1.02 , 13.54 ± 2.1 respectively) revealed a significant decrease compared to the control (31.68 ± 5.36), Whereas subgroup IIIb (37.28 ± 2.99) showed a significant increase compared to the control, while subgroup IVb (34.66 ± 6.38) showed a non-significant difference from the control. Moreover, subgroup IVa was significantly higher than subgroup IIIa, while subgroup IVb was significantly lower than subgroup IIIb (Table 1) (Histogram 1).

Immunohistochemical staining for detection of caspase-3

Immunohistochemical staining for detection of activated caspase-3 in both control subgroups and tadalafil-treated group showed scanty caspase-3 positive cells in the outer layer of the urothelium (Figure 9). Whereas, sections from subgroup IIIa revealed numerous caspase-3 positive cells in the urothelium and lamina propria (Figure 10). Moreover, sections from subgroup IIIb depicted many caspase-3 positive cells at all layers and lamina propria (Figure 11). On the other hand, sections from subgroup IVa showed some caspase-3 positive cells in the urothelium and lamina propria (Figure 12). Yet, sections from subgroup IVb revealed only a few caspase-3 positive cells in the urothelium (Figure 13).

Morphometrical analysis of the mean percentage of caspase-3 positive cells (apoptosis index) of subgroups IIIa, IIIb and IVa (25.67 ± 4.69 , 19.33 ± 3.07 , 11.91 ± 3.22 respectively) revealed a significant increase compared to the control (6.26 ± 1.02), whereas subgroup IVb (8.06 ± 2.69) recorded a non-significant difference from the control.

Moreover, subgroups IVa and IVb were significantly lower than subgroups IIIa and IIIb respectively (Table 1) (Histogram 2).

Immunohistochemical staining for detection of Ki-67

Immunohistochemical staining for detection of Ki-67 in both control subgroups and tadalafil-treated group showed few Ki-67-positive cells almost limited to the basal cell layer and lamina propria (Figure 14). Whereas, sections from subgroup IIIa revealed numerous Ki-67 positive cells particularly in the basal and intermediate layers (Figure 15). Nevertheless, sections from subgroup IIIb depicted a massive number of Ki-67 positive cells occupying the whole layers (Figure 16). On the other hand, sections from subgroup IVa revealed numerous Ki-67 positive cells particularly in the basal and intermediate layers (Figure 17). In addition, sections from subgroup IVb depicted only a few Ki-67 positive cells almost limited to the basal cell layer (Figure 18).

Morphometrical analysis of the mean percentage of Ki-67-positive cells (proliferation index) of subgroups IIIb and IVa (23.91 ± 4.81 , 17.65 ± 3.16 respectively) revealed a significant increase compared to the control (11.55 ± 2.61), whereas subgroup IIIa and IVb (12.26 ± 3.66 , 14.12 ± 3.91 respectively) recorded a non-significant difference from the control. Moreover, subgroup IVa was significantly higher than subgroup IIIa, while subgroup IVb was significantly lower than subgroups IIIb (Table 1) (Histogram 3).

Transmission electron microscopic study

Groups (I and II)

Ultrathin sections of the superficial urothelial cells of both control subgroups and tadalafil-treated group were characterized by the irregular angular contour. The apical plasma membrane had dense plaques interspersed with narrow zones of the normal membrane. The cytoplasm showed euchromatic nuclei with prominent nucleoli, apical electron-lucent fusiform vesicles and normal pleomorphic mitochondria (Figures 19,20). The superficial cells were interdigitated and held together by intact intercellular junctions in the form of zonula occludens, zonula adherens, and desmosomes between and along the lateral sides of cells (Figure 20).

Group (III)

Ultrathin sections from subgroup IIIa revealed disrupted apical plasma membrane of the superficial cells with presence of cell remnants. The cells had rarefied cytoplasm with empty spaces and cytoplasmic vacuoles. Absences of fusiform vesicles and wide intercellular spaces were observed. Some nuclear degenerative changes in the form of abnormal chromatin distribution were detected and some cells lost their nuclei (Figure 21). There were many shrunken cells in between the few remnant layers characterized by electron-dense cytoplasm and nuclear condensation adjacent to the nuclear membrane with a

severely irregular plasma membrane (Figure 22). Apoptotic bodies with condensed nuclear fragments and irregular membrane were frequently noticed in between cells in different layers (Figure 23). Sections from subgroup IIIb still depicted the loss of the characteristic angular contour of the apical plasma membrane, wide intercellular spaces, and cytoplasmic vacuoles. Nuclear changes were in the form of indented and shrunken hyperchromatic nuclei (Figure 24).

Group (IV)

Ultrathin sections from subgroup IVa revealed some superficial cells with the characteristic angular contour of the apical plasma membrane with multiple fusiform vesicles underneath. The intercellular spaces and junctions were intact. The cytoplasm of some urothelial cells contained multiple secondary lysosomes and cytoplasmic vacuoles. Most of the nuclei appeared normal with large nucleoli (Figure 25). On the other hand, sections from subgroup IVb showed that almost all cells were apparently normal with an apical angular contour. The cytoplasm contained electron-lucent fusiform vesicles, apparently normal mitochondria, and some vacuoles. Moreover, the intercellular spaces were intact with the presence of intercellular junctions. The nuclei depicted the normal appearance (Figure 26).

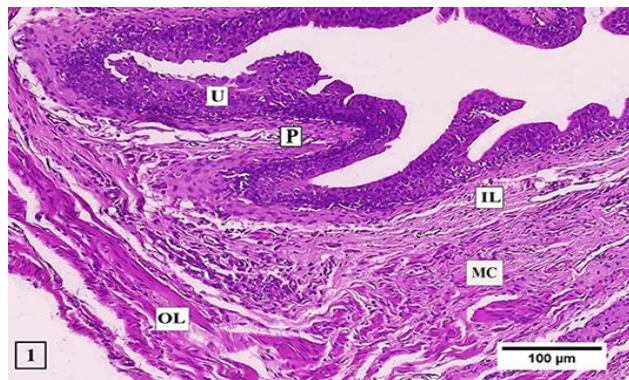


Fig. 1: A photomicrograph of a section of the urinary bladder of a control group showing the folded mucosa composed of the urothelium (U) and lamina propria (P). The muscle layer is formed of three interlaced bundles of inner longitudinal (IL), middle circular (MC), and outer longitudinal (OL). (H&Ex200, scale bar=100μ)

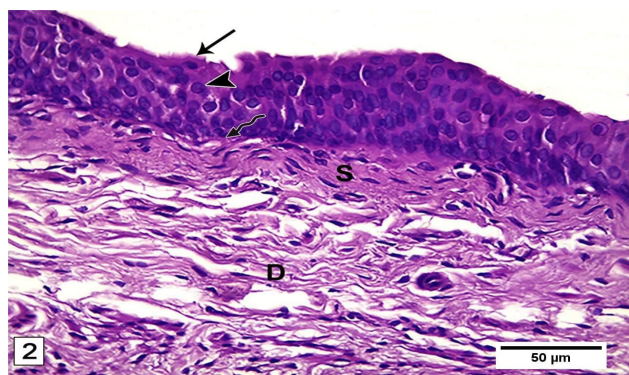


Fig. 2: A photomicrograph of a section of the urinary bladder of a control group showing the urothelium formed of surface dome-shaped cells (thin arrow), intermediate pear-shaped cells (arrowhead) and basal layer resting on basal lamina (wavy arrow). The lamina propria is differentiated into superficial dense (S) and deep loose layers (D). (H&E x400, scale bar=50μ)

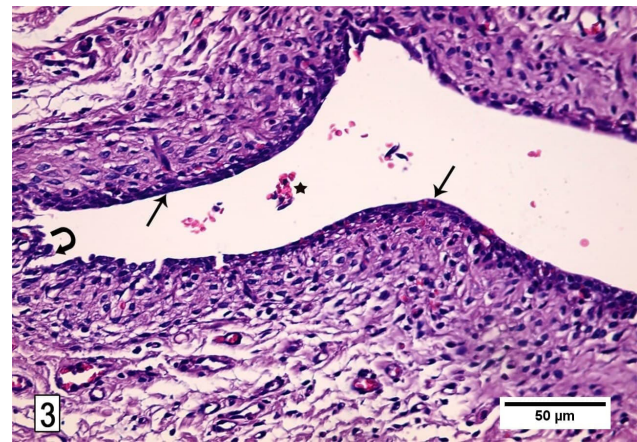


Fig. 3: A photomicrograph of a section of the urinary bladder of subgroup IIIa showing haemorrhage (star), marked decrease of the urothelium thickness to be formed of one or two rows of cells (thin arrow) with focal ulcerated areas and loss of urothelial continuity forming localized denuded areas (curved arrow). (H&E X400, scale bar=50μ)

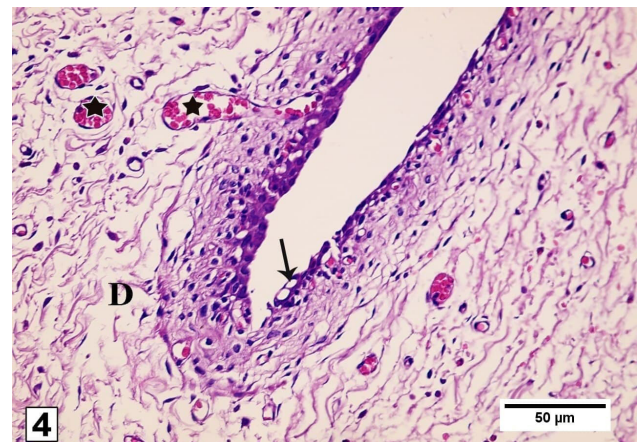


Fig. 4: A photomicrograph of a section of the urinary bladder of subgroup IIIa showing coalesced cells with vacuolated cytoplasm and deeply stained nuclei (thin arrow). The deep lamina propria appears less cellular with empty spaces (D) with dilated congested blood capillary (star). (H&E X400, scale bar=50μ)

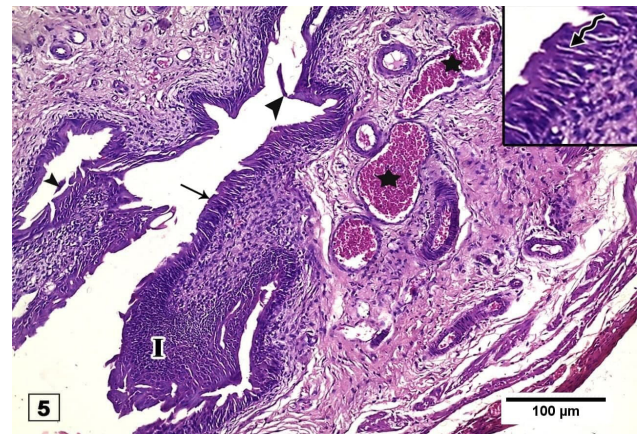


Fig. 5: A photomicrograph of a section of the urinary bladder of subgroup IIIb showing the restoration of the urothelium (thin arrow) and the presence of sloughed tissues in the lumen (arrowhead). Note the wide intercellular spaces (wavy arrow). The submucosa reveals focal areas of massive mononuclear cells infiltration (I) and dilated congested blood vessels (star). (H&E X200, scale bar=100μ); (inset, ×1000, scale bar=20 μ)

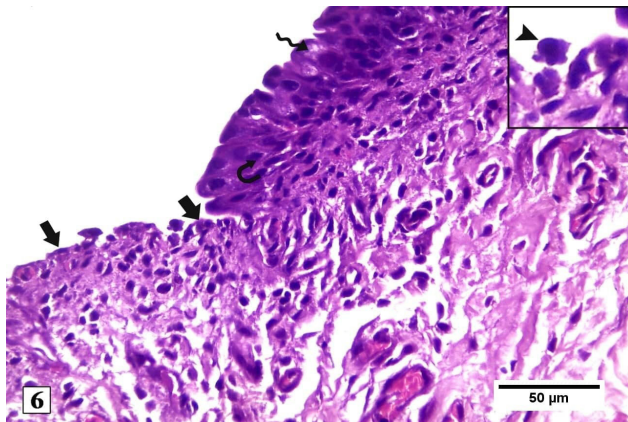


Fig. 6: A photomicrograph of a section of the urinary bladder of subgroup IIIb showing a part of the mucosa lined with few layers of urothelial cells and another ulcerated part with a denuded area of lamina propria (thick arrows). Some cells have vacuolated cytoplasm (wavy arrow) and dark pyknotic nuclei (curved arrow). Note the sloughed cells in the lumen (arrowhead). (H&E X400, scale bar=50μ) (inset, ×1000, scale bar=20 μ)

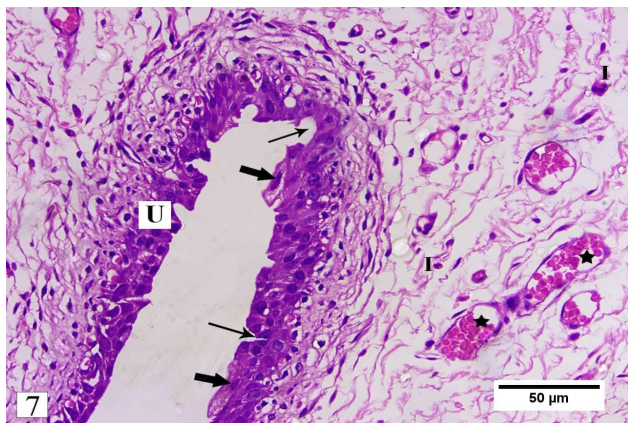


Fig. 7: A photomicrograph of a section of the urinary bladder of subgroup IVa showing an apparent decrease of the urothelial thickness (U) with focal separations and cell loss (thin arrows). Some superficial cells are enlarged with vacuolated cytoplasm (thick arrows). Submucosa shows empty spaces, dilated congested blood capillaries (star), and neutrophil infiltration (I). (H&E X400 scale bar=50μ)

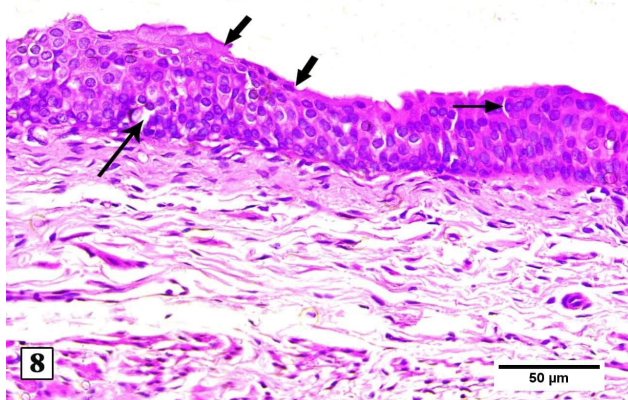


Fig. 8: A photomicrograph of a section of the urinary bladder of subgroup IVb showing restored urothelium thickness. The superficial cells show their characteristic angular contour (thick arrows) with some separations between urothelial cells (thin arrows). Notice apparently normal lamina propria. (H&E X400, scale bar=50μ)

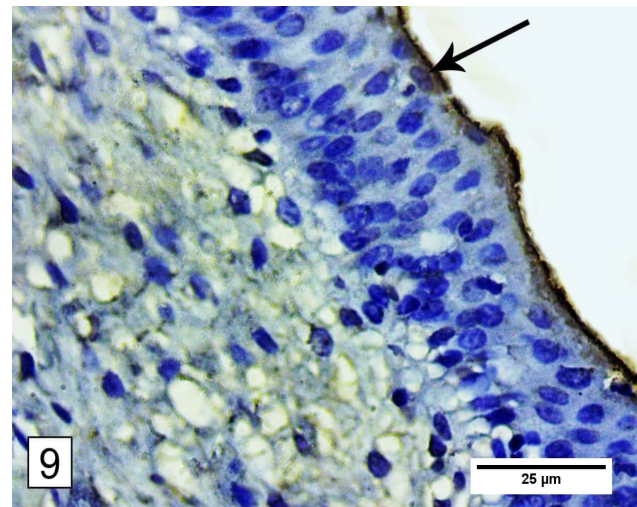


Fig. 9: A photomicrograph of a section of the urothelium of a control group showing scanty caspase-3 positive cells in the outer layer of the urothelium (thin arrow). (caspase-3 X1000, scale bar=25 μ)

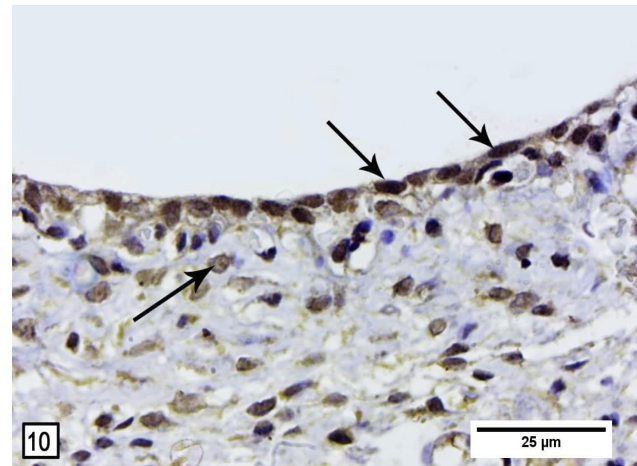


Fig. 10: A photomicrograph of the urothelium of subgroup IIIa showing numerous caspase-3 positive cells in the urothelium and lamina propria (thin arrows). (caspase-3 X1000, scale bar=25 μ)

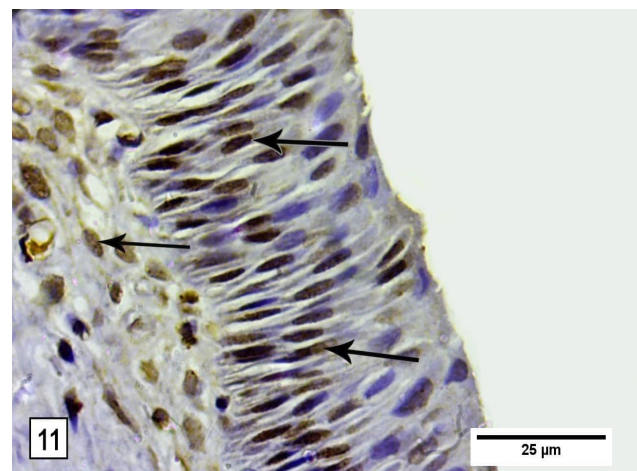


Fig. 11: A photomicrograph of the urothelium of subgroup IIIb showing many caspase-3 positive cells at all layers of urothelium and lamina propria (thin arrows). (caspase-3 X1000, scale bar=25 μ)

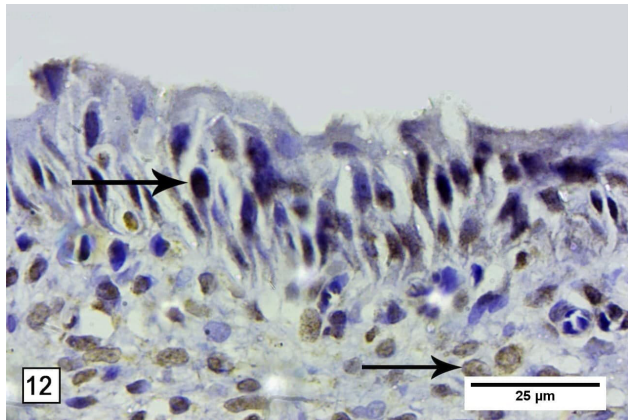


Fig. 12: A photomicrograph of the urothelium of subgroup IVa showing some caspase-3 positive cells in the urothelium and lamina propria (thin arrows). (caspase-3 X1000, scale bar=25 μ)

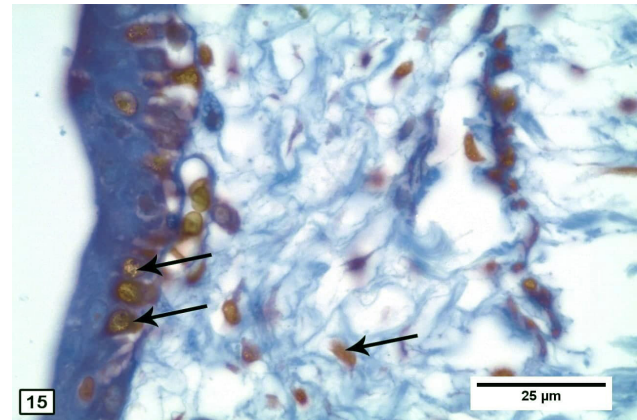


Fig. 15: A photomicrograph of the urothelium of subgroup IIIa showing several Ki-67 positive cells in the basal and intermediate layers besides the lamina propria (thin arrows). (Ki-67 X 1000, scale bar=25 μ)

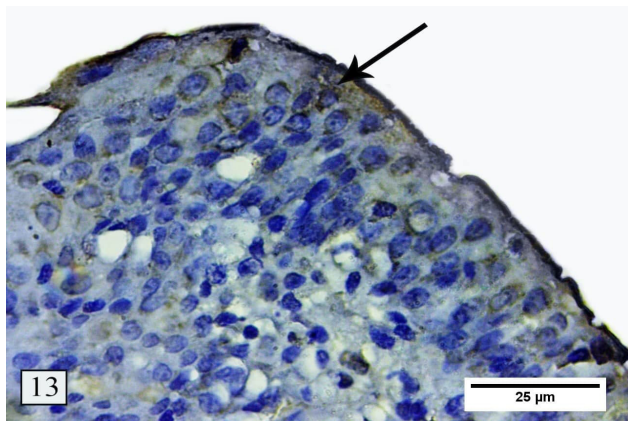


Fig. 13: A photomicrograph of the urothelium of subgroup IVb showing few caspase-3 positive cells in the urothelium (thin arrows). (caspase-3 X1000, scale bar=25 μ)

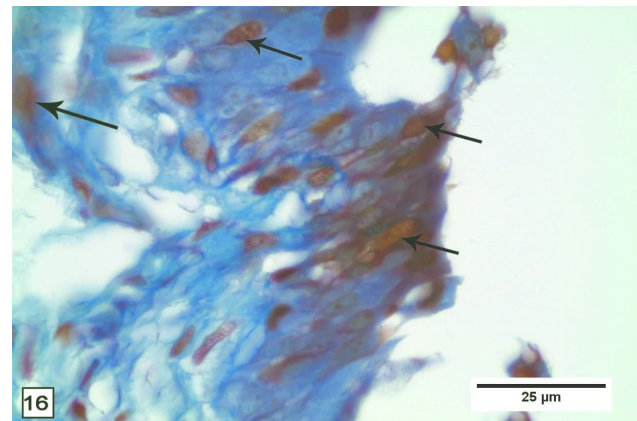


Fig. 16: A photomicrograph of the urothelium of subgroup IIIb showing a massive number of Ki-67 positive cells occupying the whole layers reaching up to the superficial layer (thin arrows). (Ki-67 X 1000, scale bar=25 μ)

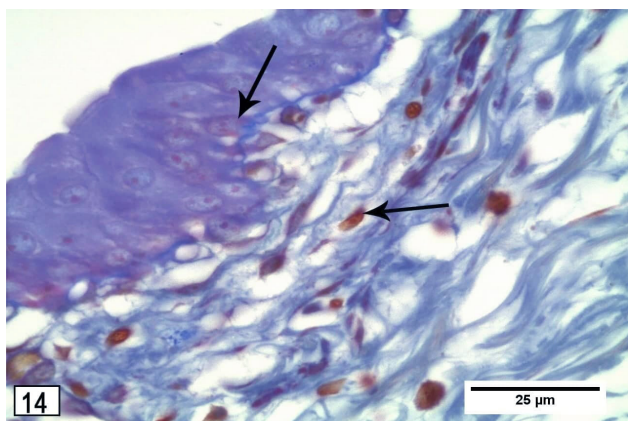


Fig. 14: A photomicrograph of a section of the urothelium of a control group showing few ki-67 positive cells mainly in the basal layer of the urothelium and lamina propria (thin arrows). (Ki-67 X 1000, scale bar=25 μ)

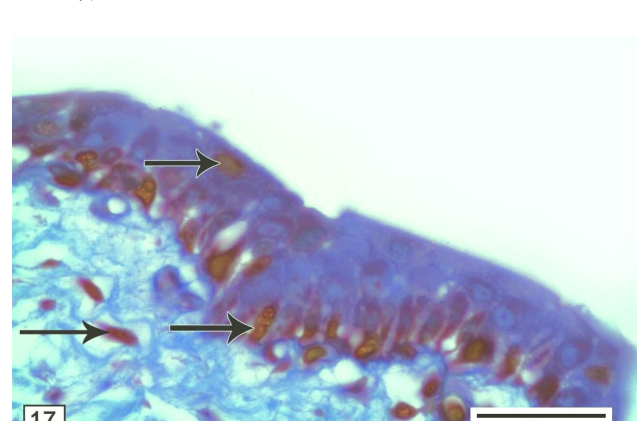


Fig. 17: A photomicrograph of the urothelium of subgroup IVa showing numerous Ki-67 positive cells limited to basal and intermediate layers (thin arrows). (Ki-67 X 1000, scale bar=25 μ)

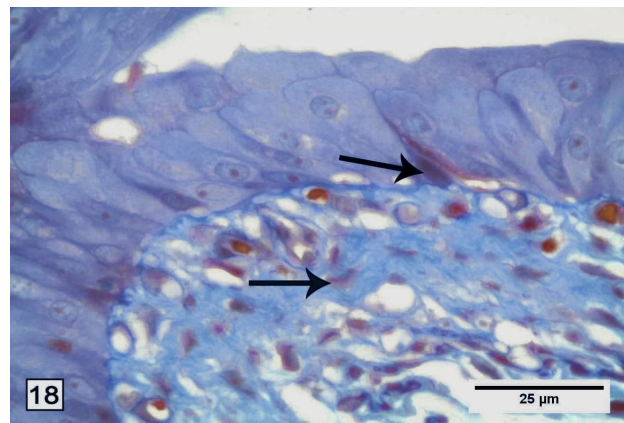
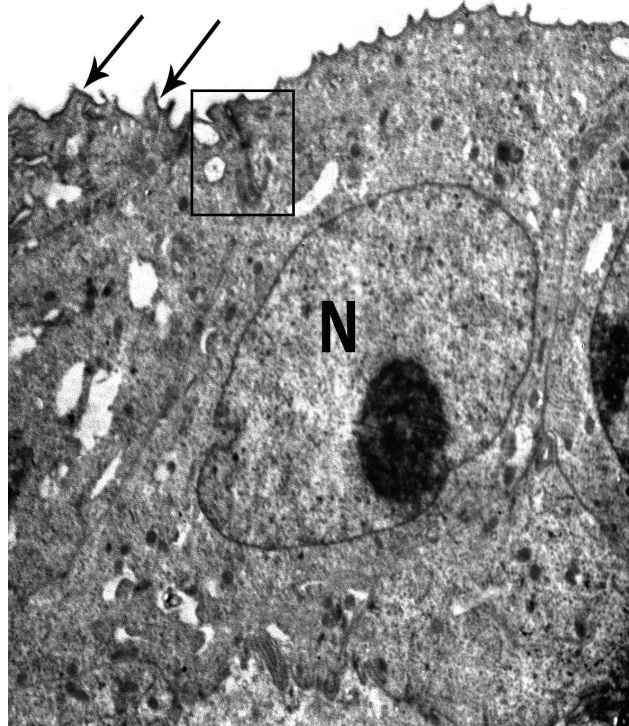


Fig. 18: A photomicrograph of the urothelium of subgroup IVb showing few Ki-67 positive cells limited to the basal layer and lamina propria (thin arrows). (Ki-67 X 1000, scale bar=25 μ)



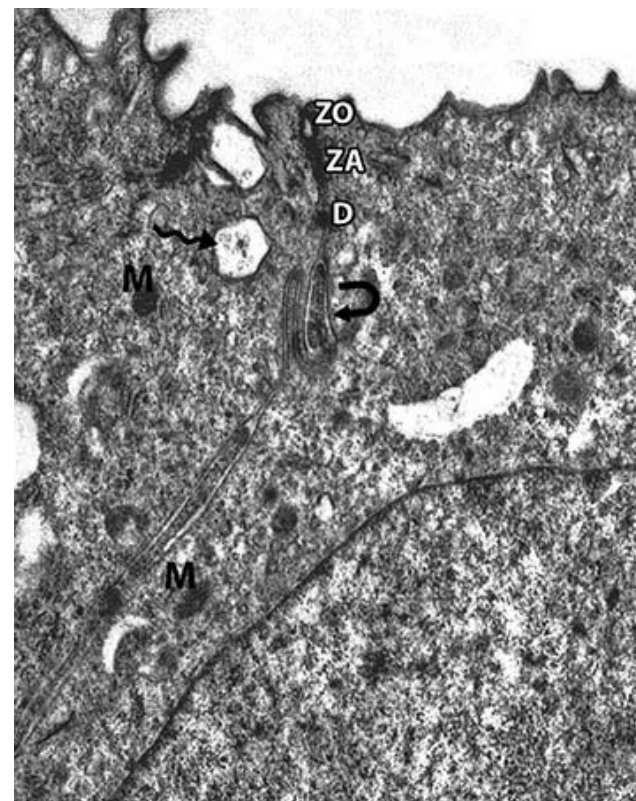
Dr Sherine Elabd UB2002
Print Mag: 11700x @ 7.0 in
TEM Mode: Imaging

2 microns
HV=2000.0kV
Direct Mag: 2000x

19



Fig. 19: An electron micrograph of the urothelium from a control group showing irregular dense plaques at the apical surface (thin arrow) and a nucleus exhibiting normally dispersed chromatin with prominent nucleolus (N). TEM × 2000



Dr Sherine Elabd UB2003
Print Mag: 29200x @ 7.0 in
TEM Mode: Imaging

500 nm
HV=2000.0kV
Direct Mag: 5000x

20



Fig. 20: A higher magnification of the previous figure showing a minimal intercellular space with interdigitation (curved arrow) and intact intercellular junctions formed of zonula occludens (ZO), zonula adherens (ZA) and desmosome (D). The cytoplasm contains normal pleomorphic mitochondria (M) and multiple fusiform electron-lucent vesicles (wavy arrow).TEM × 5000.

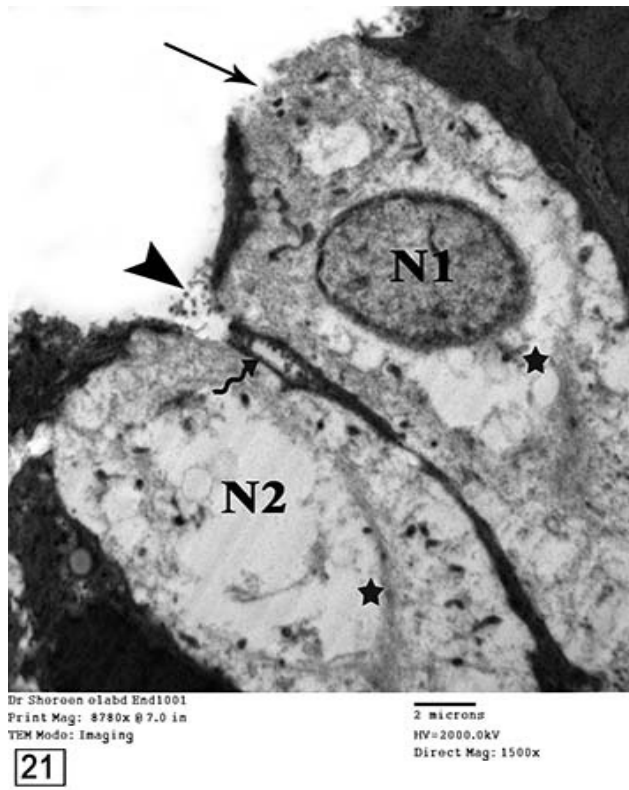


Fig. 21: An electron micrograph of subgroup IIIa showing a focal disruption of the apical plasma membrane (thin arrow), cell remnants (arrowhead), absence of fusiform vesicles and wide intercellular space (wavy arrow). The cytoplasm appears rarefied with empty spaces (star). Note a cell with a nucleus exhibiting a decreased chromatinic rim (N1) while the other cell lost its nucleus (N2).TEM × 1500.

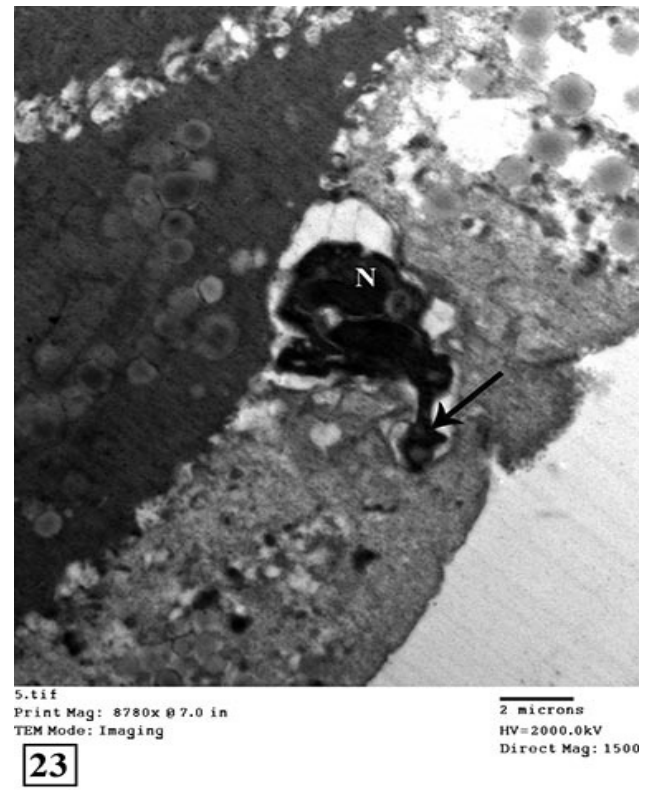


Fig. 23: An electron micrograph of subgroup IIIa showing an apoptotic body in between urothelial cells. It has an irregular membrane (thin arrow) and contains fragments of the nucleus with condensed chromatin (N). TEMx1500

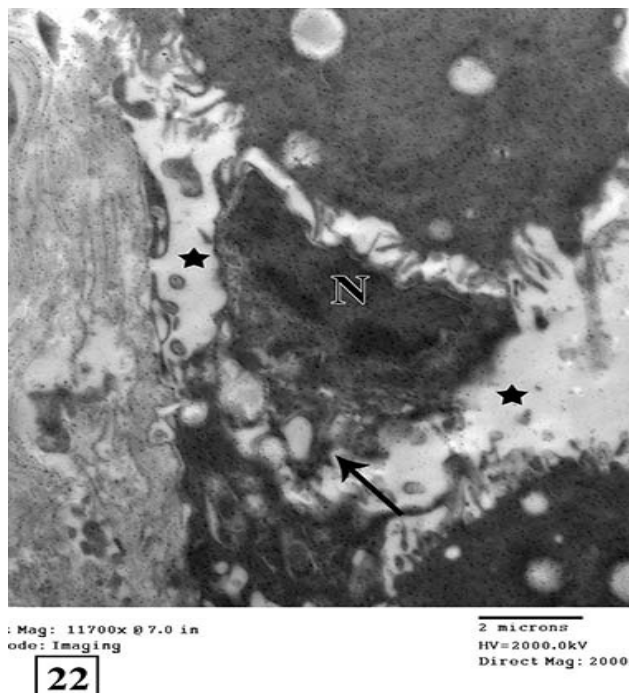


Fig. 22: An electron micrograph of subgroup IIIa showing a shrunken cell separated from the other surrounding cells (stars). The plasma membrane is severely irregular (arrow), the cytoplasm is electron-dense and the nucleus is indented with chromatin condensation adjacent to the nuclear membrane (N).TEM × 2000.

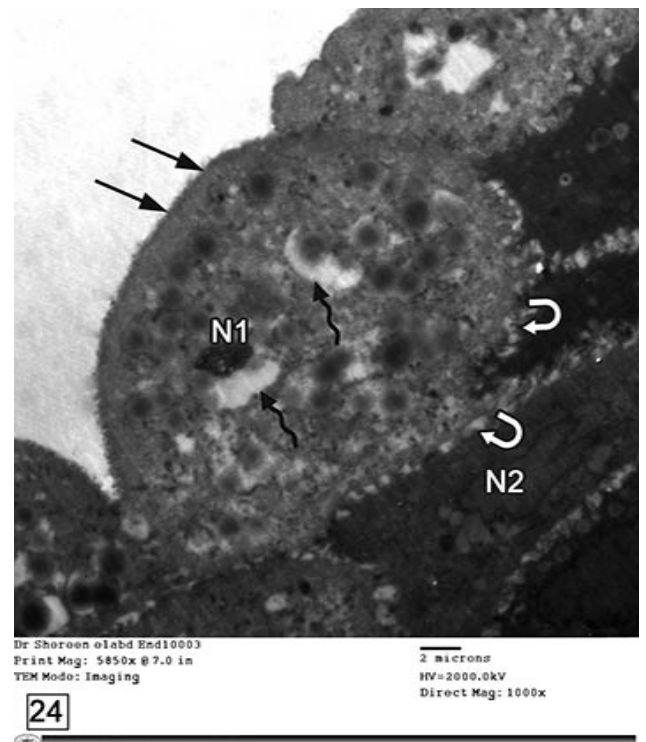


Fig. 24: An electron micrograph from subgroup IIIb showing superficial urothelial cells with loss of the characteristic angular contour (thin arrows), wide intercellular spaces (curved arrows) and cytoplasmic vacuoles (wavy arrows). Note the hyperchromatic shrunken nucleus (N1) and the other indented one (N2).TEM × 1000.

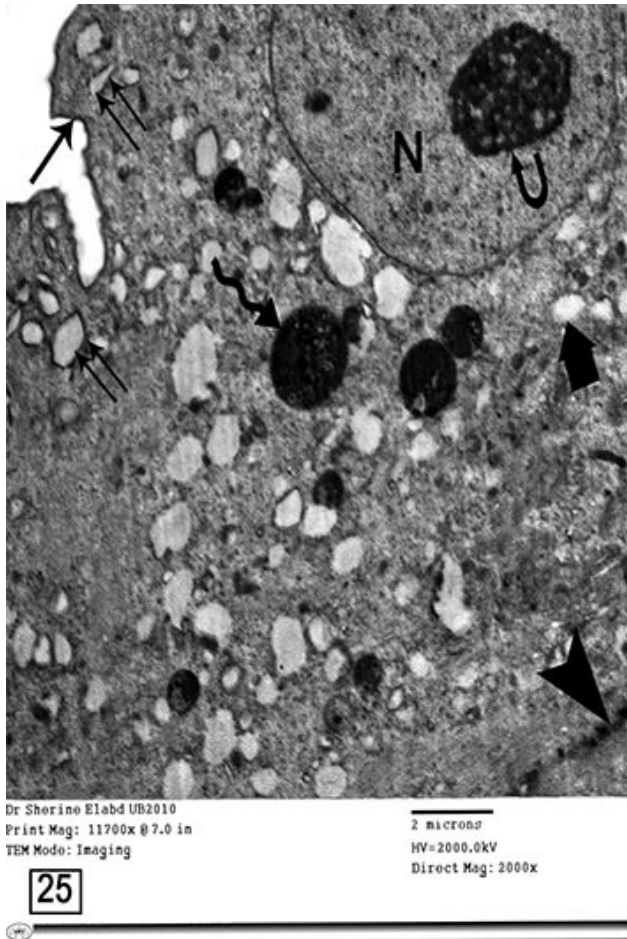


Fig. 25: An electron micrograph of the urothelial cells from subgroup IVa showing the characteristic angular contour (thin arrow), fusiform vesicles (double arrows) and intact intercellular junctions (arrowhead). The cytoplasm contains secondary lysosomes (wavy arrow) and cytoplasmic vacuoles (thick arrow). The nucleus (N) appears normal with a large nucleolus (curved arrow). TEMX2000

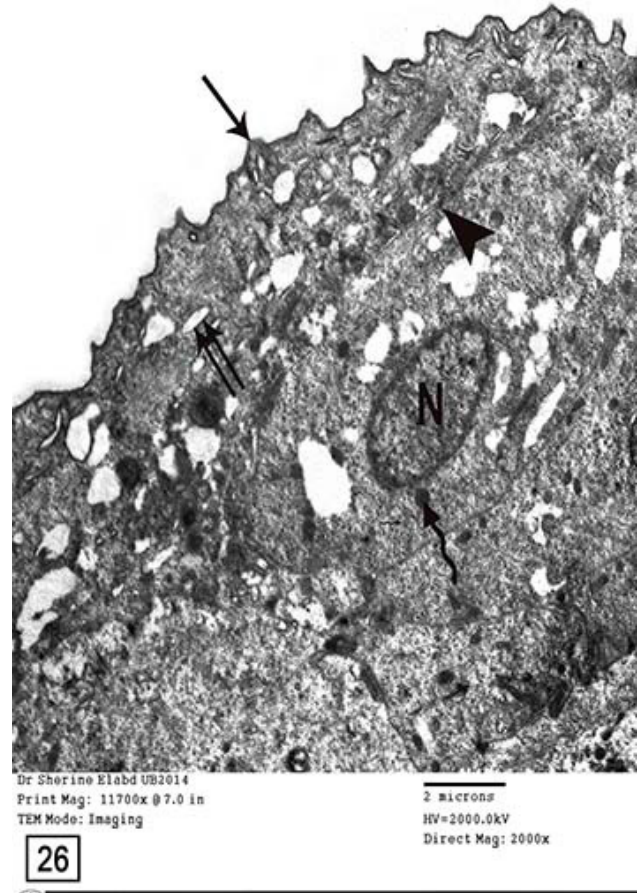
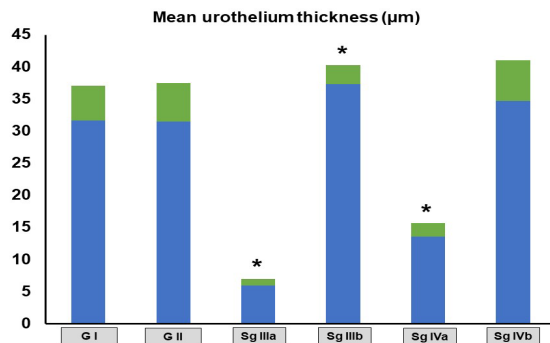


Fig. 26: An electron micrograph of the urothelial cells of subgroup IVb showing angular contour of the apical plasma membrane (thin arrow), fusiform vesicles (double arrows) and normal shaped mitochondria (wavy arrow). Notice an apparently normal nucleus (N) and intact intercellular junction (arrowhead). TEMX2000

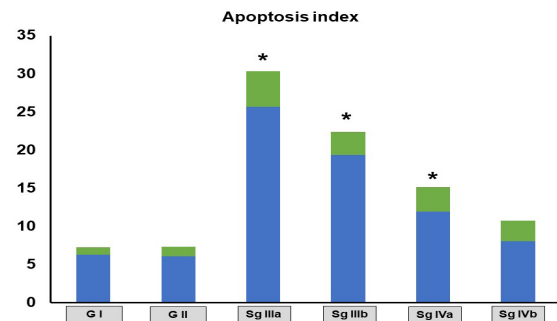
Table 1: Morphometrical analysis of the different study groups

Parameters	Group I	Group II	Group III		Group IV	
			Subgroup IIIa	Subgroup IIIb	Subgroup IVa	Subgroup IVb
Mean urothelium thickness (μm)	31.68 \pm 5.36	31.49 \pm 5.96	5.94 \pm 1.02 ^{a,b}	37.28 \pm 2.99 ^{a,b}	13.54 \pm 2.1 ^{a,b,c}	34.66 \pm 6.38 ^d
Apoptosis index	6.26 \pm 1.02	6.11 \pm 1.19	25.67 \pm 4.69 ^{a,b}	19.33 \pm 3.07 ^{a,b}	11.91 \pm 3.22 ^{a,b,c}	8.06 \pm 2.69 ^d
Proliferation index	11.55 \pm 2.61	11.862.09	12.26 \pm 3.66	23.91 \pm 4.81 ^{a,b}	17.65 \pm 3.16 ^{a,b,c}	14.12 \pm 3.91 ^d

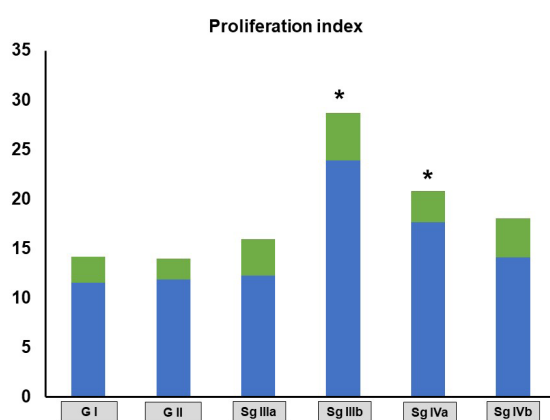
Data is expressed as mean \pm standard deviation, a indicates significance versus group I, b indicates significance versus group II, c indicates significance versus subgroup IIIa, d indicates significance versus subgroup IIIb.



Histogram 1: Morphometric analysis of mean urothelium thickness of the urinary bladder (μm) * indicates significance versus the control group.



Histogram 2: Morphometric analysis of the mean area percentage (%) of caspase-3-positive cells (Apoptosis index), * indicates significance versus the control group.



Histogram 3: Morphometric analysis of the mean area percentage (%) of Ki67-positive cells (Proliferation index). * indicates significance versus the control group.

DISCUSSION

HC commonly develops in patients receiving CYP as a part of their treatment against cancer and autoimmune diseases^[1]. The urothelial damage done by CYP is mainly due to the passage of the active product acrolein into the urinary bladder producing a redox imbalance in the urothelium^[31].

CYP treatment causes massive destruction of the urothelium by both necrosis and apoptosis, followed by regeneration of the surviving cells^[32]. It happened similarly in the current work after 1 day of a single injection of CYP (subgroup IIIa). The histological findings were in the form of haemorrhage and a noticeable decrease of urothelium thickness with numerous ulcerations and denudation with affection of the lamina propria. Most cells had the characters of necrosis in the form of destruction of the apical plasma membrane, cytoplasmic vacuoles, karyolysis, and widening of intercellular spaces.

After 10 days from CYP injection (subgroup IIIb), despite the urothelium was formed of many different layers; focal denuded areas were still observed, also the cytoplasm was vacuolated with dark hyperchromatic nuclei. In both periods of this group, the mucosa appeared oedematous with dilated congested blood vessels and massive inflammatory cellular infiltrations. Our results were consistent with several studies^[23,33-35] further more explained as a single injection of CYP triggers an inflammatory reaction in the urinary bladder^[10,11].

In the current work, the apoptotic index revealed a highly significant increase in subgroups IIIa and IIIb compared to control. The apoptotic index was elevated at day 1 and declined at day 10; it confirms that apoptosis comes early after necrosis to play a vital role in cell elimination. Apoptosis usually occurs near the areas of necrosis to permit the removal of the damaged cells that do not undergo necrosis^[10,17]. This explanation is demonstrated by active caspase-3 immunohistochemistry and confirmed also by electron microscopy. A plentiful number of apoptotic bodies as well as shrunken cells with irregular

cell membrane and condensed fragmented nuclei were noticed among the necrotic cells in all cell layers. Also, caspase-3 positive cells have been seen in all cell layers, suggesting that cells of all urothelial layers are responsive to apoptotic stimuli^[17].

The immunolocalization of acrolein in the wall of the urinary bladder in rats has been documented after CYP injection; it was consistent with the elevation of IL-6 in both serum and bladder tissue^[23]. Moreover, the elevation of the inflammatory cytokines IL-1 β , TNF α , and platelet-activating factor (PAF) were also recorded to be implicated in the pathophysiology of CYP-induced HC^[2,35,36].

Souza-Filho *et al.*,^[37] observed an increase in the inducible Nitric oxide synthase (iNOS) with a concomitant decrease of the constitutive NOS after CYP injection leading to release of a large amount of NO over a long duration by immune cells inducing a cytotoxic effect. Acrolein raises ROS by catalyzing the reaction of glutathione to glutathionyl-propionaldehyde (GTPD) that activates nuclear factor kappa B (NF- κ B) apoptotic pathway. NF- κ B binds with several enzymes, particularly xanthine oxidase and aldehyde dehydrogenase, forming superoxide radicals that react with NO producing peroxynitrite radicals and subsequently commit cells to necrosis or apoptosis^[38].

In the current work, the CYP-TAD treated group showed amelioration of the previous histological findings. After one day (subgroup IVa); the thickness of the urothelium decreased but not as much as subgroup IIIa, in addition to a few localized areas of cell loss with no evident denuded areas. The submucosa showed congested blood vessels with mild neutrophil infiltration. After ten days (subgroup IVb), the thickness of the urothelium appeared normal and the cells exhibited their normal features, in addition, the mucosa seemed normal with no congested blood vessels or inflammatory cells.

Subgroup IVa revealed a significant increase in apoptotic index compared to control, but still lower than subgroups IIIa and IIIb, although subgroup IVb revealed a non-significant difference compared to the control. This was in accordance with Baek *et al.*^[42] who found that 10 mg/kg of TDF repressed the apoptotic neuronal cell death and boost cell proliferation in the hippocampus of maternal-separated young rats, this was in addition to the previously mentioned studies about the anti-apoptotic activity of TAD on different organs^[39-41].

The predictable mechanism of the anti-inflammatory effect of TAD on HC is the augmentation of NO/cGMP signaling pathway that induces smooth muscle cell relaxation resulting in increased blood perfusion in the bladder^[43-45]. Moreover, the increased cGMP and the activation of mitochondrial potassium ATP (ATPK+) channels have a direct and indirect anti-apoptotic effect through a variety of signaling pathways, as activation of protein kinase C (PKC) and (PKG). Opening of mitochondrial ATPK+ channel may prohibit apoptosis as it inhibits the mitochondrial accumulation of Ca⁺, and

also by preserving the inner mitochondrial membrane potential^[41,46]. Also, it has been shown that sildenafil induces an increase of cytochrome-c secretion, up-regulation of Bcl2/Bax ratio, and decrease of apoptotic protease activating factor-1 (APAF1) level through NO signaling pathway having an important role in inhibiting apoptosis^[41,47,48].

Many studies attributed the anti-apoptotic properties of TAD to ROS inhibition^[49] and also the block of the development of inflammatory cytokines and reduction leukocyte aggregation^[50,51]. Furthermore, TAD has the ability to inhibit the secretion of pro-inflammatory cytokine IL-8 in human myofibroblasts and endothelial cells^[52,53]. PDF5 inhibitors reduce both the activity and the expression of NADPH oxidase resulting in the inhibition of superoxide production in endothelial and smooth muscle cells^[49].

In the current study, the proliferation index revealed a significant increase in subgroups IIIb and IVa compared to control, while subgroups IIIa and IVb revealed a non-significant change compared to control. While Ki-67 positive cells in subgroup IIIa were mainly limited in the basal and intermediate layers, they were occupying all the layers in subgroup IIIb in contrast to the control urothelium, where only the basal cells regenerate. Detection of proliferation index by Ki-67 expression was working hand in hand with the estimation of the urothelial thickness. There was a significant decrease in subgroups IIIa and IVa compared to control, on the other hand, subgroup IIIb revealed a significant increase compared to control. Moreover the urothelial thickness of subgroup IVa was significantly higher than subgroup IIIa, while subgroup IVb was significantly lower than subgroup IIIb.

In this study, the differentiation process was reflected by the ultrastructural findings that revealed absence of dense plaques in the superficial luminal cells in group III, while the characteristic angular contour appeared in some cells in subgroup IVa and almost all cells of subgroup IVb. It appears that, following TAD treatment, the differentiation process was faster than CYP group, as all luminal cells had already reached the differentiated state after 10 days.

Recently, several studies mentioned that TAD shortens the time of healing and fastens the regeneration period in different organs^[54-56]. Hoke *et al.*,^[57] found that intra-cardiac injection of preconditioned adipose stem cells (ASCs) with PDE5 inhibitor-sildenafil helped regeneration and improved the survival of cardiomyocytes following myocardial infarction. Additionally, it has been mentioned that administration of different doses of sildenafil accelerated the regeneration and the mitotic rate of hepatocytes after partial hepatectomy^[58]. Sildenafil also significantly enhanced the release of growth factors (GFs) as vascular endothelial growth factor (VEGF), beta fibroblast growth factor (b-FGF), insulin-like growth factor (IGF), and angioprotein-1. These GFs would stimulate urothelium proliferation, blood vessel formation/

maturation, regeneration of neuromuscular junction, and smooth muscle layer reorganization^[59].

CONCLUSION

The results of this study showed that TAD (PDE-5 inhibitor) co-treatment ameliorated HC induced by CYP in rats. TAD, at a dose (10 mg/kg), inhibited apoptosis, controlled proliferation of urothelial cells, and also stimulated their terminal differentiation faster during regeneration and restoration of the urothelium and the underlying lamina propria of the urinary bladder.

RECOMMENDATIONS

Further studies are required to elucidate the protective effect of TAD on CYP-induced HC to be included more safely in the chemotherapy regimens of cancer patients and patients complaining of autoimmune diseases.

CONFLICT OF INTERESTS

There are no conflicts of interest.

REFERENCES

1. Ayhanci A., Yaman S., Sahinturk V., Uyar R., Bayramoglu G., Senturk H., Altuner Y. *et al.*, Protective Effect of Seleno-L-Methionine on Cyclophosphamide-Induced Urinary Bladder Toxicity in Rats. *Biological trace element research*. 2010; 134:98–108. DOI: 10.1007/s12011-009-8458-y.
2. Dantas ACB, Batista-Júnior FFA, Macedo LF, Mendes MNC, Azevedo IM, Medeiros AC. Protective effect of simvastatin in the cyclophosphamide-induced hemorrhagic cystitis in rats. *Acta Cir Bras*. [serial on the Internet] 2010; Jan-Feb;25(1). Available from URL:<http://www.scielo.br/acb>.
3. Whalen K., Finkel R. (ed) and Panavelil T. (ed). *Pharmacology*. Lippincott Illustrated Reviews. 6th Ed. Wolter Kluwer. China. Philadelphia. Baltimore. New York. London. 2015; Unit VII, chapter 46:600-601. ISBN.9781451191776 1451191774.
4. Matz EL and Hsieh MH: Review of Advances in Uroprotective Agents for Cyclophosphamide- and Ifosfamide-induced Hemorrhagic Cystitis. *UROLOGY*. 2017; 100: 16–19. DOI: <https://doi.org/10.1016/j.urology.2016.07.030>.
5. Colvin OM: An overview of cyclophosphamide development and clinical applications. *Curr Pharm Des*. 1999; 5:555-60.5) Brock N and Pohl J: The Development of MESNA for Regional detoxification. *Cancer Treat Rev*. 1983; 10 (1):33-43. DOI:10.1016/s0305-7372(83)80005-x
6. Haldar S, Dru C, Bhowmick NA: Mechanisms of hemorrhagic cystitis. Review Article. *Am J Clin Exp Urol*. 2014;2(3):199-208.6) Watson NA, Notley RG. Urological Complications of cyclophosphamide. *Br J Urolo*. 1973; 45:606.

7. Ribeiro RA, Freitas HC, Campos MC, Santos CC, Figueiredo FC, Brito GA, Cunha FQ: Tumor necrosis factor-alpha and interleukin-1beta mediate the production of nitric oxide involved in the pathogenesis of ifosfamide induced hemorrhagic cystitis in mice. *J Urol.* 2002;167:2229-34.
8. Türk G, Ceribaşı AO, Sakin F, Sönmez M, Ateşşahin A: Antiperoxidative and antiapoptotic effects of lycopene and ellagic acid on cyclophosphamide-induced testicular lipid peroxidation and apoptosis. *Reprod Fertil Dev* 2010;22:587–596.
9. Özcan A, Korkmaz A, Oter S, Coskun O: Contribution of flavonoid antioxidants to the preventive effect of MESNA in cyclophosphamide-induced cystitis in rats. *Arch Toxicol.* 2005; 79:461–465.
10. Zupančič D, Jezernik K and Vidmar G: Effect of melatonin on apoptosis, proliferation and differentiation of urothelial cells after cyclophosphamide treatment. *Journal of Pineal Research.* 2008; 44:299–306.
11. Mahmoudi N, Eftekharzadeh S, Golmohammadi M, Khorramirouz R, Hashemi J, Kashani Z, Alijani M, Hamidieh AA, Kajbafzadeh AM: Alleviation of Cyclophosphamide-induced Hemorrhagic Cystitis by Dietary Pomegranate: A Comparative Experimental Study With Mesna. *J Pediatr Hematol Oncol.* 2018; Nov;40(8):609-615. doi: 10.1097/MPH.0000000000001203.
12. Giuliano F, Ückert S, Maggi M, Birder L, Kissel J, Viktrup L: The Mechanism of Action of Phosphodiesterase Type 5 Inhibitors in the Treatment of Lower Urinary Tract Symptoms Related to Benign Prostatic Hyperplasia. *European urology.* 2013; 63(3):506–516. <http://dx.doi.org/10.1016/j.eururo.2012.09.006>.
13. Yokoyama O, Igawa Y, Takeda M, Yamaguchi T, Murakami M and Viktrup L: Tadalafil for lower urinary tract symptoms secondary to benign prostatic hyperplasia: a review of clinical data in Asian men and an update on the mechanism of action. *Ther Adv in Uro.* 2015, 7(5) 249–264. doi: 10.1177/1756287215589238.
14. Zarifpour M, Nomiya M, Sawada N and Andersson K-E: Protective Effect of Tadalafil on the Functional and Structural Changes of the Rat Ventral Prostate Caused by Chronic Pelvic Ischemia. *The Prostate.* 2015; 75:233-241. DOI 10.1002/pros.22909.
15. Morelli A, Sarchielli E, Comeglio P, Filippi S, Mancina R, Gacci M, Vignozzi L, Carini M, Vannelli GB, and Maggi M: Phosphodiesterase Type 5 Expression in Human and Rat Lower Urinary Tract Tissues and the Effect of Tadalafil on Prostate Gland Oxygenation in Spontaneously Hypertensive Rats. *J Sex Med.* 2011;8:2746–2760. DOI: 10.1111/j.1743-6109.2011.02416.x
16. Ustün H, Akgül KT, Ayyıldız A, Yağmurdu H, Nuhuğlu B, Karagüzel E, Oğuş E, Germiyanoglu C: Effect of phosphodiesterase-5 inhibitors on apoptosis and nitric oxide synthases in testis torsion: an experimental study. *Pediatr Surg Int* 2008;24:205–211.
17. Jezernik K, Romih R, Mannherz HG *et al.* Immunohistochemical detection of apoptosis, proliferation and inducible nitric oxide synthase in rat urothelium damaged by cyclophosphamide treatment. *Cell Biol Int* 2003; 27:863–869.
18. Lee G, Romih R, and Zupančič D: Cystitis: From Urothelial Cell Biology to Clinical Applications. *BioMed Research International.* 2014, Article ID 473536. <http://dx.doi.org/10.1155/2014/473536>
19. Romih R, Koprivec D, Martincic S, and Jezernik K: Restoration of the rat urothelium after cyclophosphamide treatment. *Cell Biology International.* 2001, 25(6): 531–537. <https://doi.org/10.1006/cbir.2000.0658>
20. Elmore S: Apoptosis: A Review of Programmed Cell Death. *Toxicol Pathol.* 2007; 35(4): 495–516. <https://doi.org/10.1080/01926230701320337>.
21. Badawi MA, El-Sharkawy S, Abbas NF, Abdel-Aal WE: Image analysis and Ki-67 expression in urothelial dysplasia and Carcinoma. *Journal of The Arab Society for Medical Research.* 2018, 13:144–150.
22. Scholzen T, Gerdes J (2020): The Ki-67 protein: from the known and the unknown. *J Cell Physiol* 182: 311-322. Doi:10.1002/(SICI)1097-4652(200003)182:3<311::AID-JCP1>3.0.CO;2-9
23. Yigitaslan S, Ozatik O, Ozatik FY, Erol K, Sirmagul B and Baseskioglu AB (2014): Effects of Tadalafil on Hemorrhagic Cystitis and Testicular Dysfunction Induced by Cyclophosphamide in Rats. *Urol Int.*93:55–62. DOI: 10.1159/000352095
24. Gaertner, D.J., Hallman, T.M., Hankenson, F.C. and Batchelder, M.A. (2008): Anesthesia and Analgesia for Laboratory Rodents. In *Anesthesia and Analgesia in Laboratory Animals*, 2nd ed. (Fish, R.E., Brown, M.J., Danneman, P.J., and Karas, A.Z. ed.), pp.239-297, Academic Press, New York.
25. Suvarna S, Layton Ch, Bancroft J: Bancroft's Theory and Practice of Histological Techniques. 8th ed. Elsevier. China. 2019. Chapter 10 and 19. <https://doi.org/10.1016/B978-0-7020-6864-5.01001-X>
26. Buchwalow IB and Böcker W (2010): Immunohistochemistry: Basics and Methods. Chapter 2, P:22. Springer-Verlag Berlin Heidelberg. ISBN978-3-642-04608-7. DOI <https://doi.org/10.1007/978-3-642-04609-4>

27. Kuo J. Electron microscopy: methods and protocols. 2nd ed. Totowa, New Jersey: Humana Press Inc.; 2007. p. 19. ISSN 1064-3745. Doi 10.1007/978-1-59745-294-6
28. Erzar E, Kos MK, Orc KL, Veranič P and Erman A (2020): Does the Urothelium of Old Mice Regenerate after Chitosan Injury as Quickly as the Urothelium of Young Mice? *Int. J. Mol. Sci.* 21(10), 3502; <https://doi.org/10.3390/ijms21103502>.
29. Walaa M. Elwan and Marwa A. A. Ibrahim (2019) Effect of tartrazine on gastric mucosa and the possible role of recovery with or without riboflavin in adult male albino rat. *Egypt. J. Histol.* 42(2): 482-495. doi: 10.21608/ejh.2019.6312.1043.
30. Dawson, B., Trapp, R.G., 2004. Basic & Clinical Biostatistics, in: Basic & Clinical Biostatistics. Lange Medical Books / McGraw-Hill Medical Publishing Division, pp. 162–189.
31. Cox PJ (1979). Cyclophosphamide cystitis-identification of acrolein as the causative agent. *Biochemical Pharmacology*, 28:2045-2049.
32. Jezernik K, Romih R, Mannherz HG, Koprivec D (2003): Immunohistochemical detection of apoptosis, proliferation and inducible nitric oxide synthase in rat urothelium damaged by cyclophosphamide treatment. *Cell Biology International* 27 (2003) 863–869 doi:10.1016/S1065-6995(03)00175-6
33. Arafa HM: Uroprotective effects of curcumin in cyclophosphamide-induced haemorrhagic cystitis paradigm. *Basic Clin Pharmacol Toxicol* 2009; 104: 393–399.
34. Barut EN, Engin S, Barut B, Kaya C, Kerimoglu G, Ozel A Kadioglu M (2019): Uroprotective effect of ambroxol in cyclophosphamide-induced cystitis in mice. *International Urology and Nephrology*. doi.org/10.1007/s11255-019-02128-y.
35. Morais M.M., Belarmino-Filho J.N., Brito G.A.C. and Ribeiro R.A. (1999): Pharmacological and histopathological study of cyclophosphamide-induced hemorrhagic cystitis - comparison of the effects of dexamethasone and Mesna. *Brazilian Journal of Medical and Biological Research.* 32: 1211-1215. doi.org/10.1590/S0100-879X1999001000006.
36. Gomes TNA, Santos CC, Souza-Filho, MVP, Cunha FQ & Ribeiro RA (1995). Participation of TNF- α and IL-1 in the pathogenesis of cyclophosphamide-induced hemorrhagic cystitis. *Brazilian Journal of Medical and Biological Research*, 28:1103-1108.
37. Souza-Filho MVP, Lima MVA, Pompeu MML, Ballejo G, Cunha FQ & Ribeiro RA (1997). Involvement of nitric oxide in the pathogenesis of cyclophosphamide-induced hemorrhagic cystitis. *American Journal of Pathology*, 150: 247-256
38. Haldar S, Dru CH, Bhowmick N (2014): Mechanisms of hemorrhagic cystitis. *Am J Clin Exp Urol* 2014;2(3):199-208. ISSN:2330-1910/AJCEU0002263
39. Koka S, Das A, Zhu SG, Durrant D, Xi L, Kukreja RC: Long-acting phosphodiesterase-5 inhibitor tadalafil attenuates doxorubicin-induced cardiomyopathy without interfering with chemotherapeutic effect. *J Pharmacol Exp Ther* 2010; 334: 1023–1030.
40. Erol B, Tokgoz H, Hanci V, Bektas S, Akduman B, Yencilek F, Mungan G, Mungan A: Vardenafil reduces testicular damage following ischemia/reperfusion injury in rats. *Kaohsiung J Med Sci* 2009; 25: 374–380.
41. Bektas S, Karakaya K, Can M, Bahadir B, Guven B, Erdogan N, Ozdamar SO (2016): The effects of tadalafil and pentoxifylline on apoptosis and nitric oxide synthase in liver ischemia/reperfusion injury. *The Kaohsiung Journal of Medical Sciences* • June 2016. 32(7):339-347. doi.org/10.1016/j.kjms.2016.05.005
42. Baek SB, Bahn G, Moon SJ, Lee J, Kim KH, Ko IG, *et al.* The phosphodiesterase type-5 inhibitor, tadalafil, improves depressive symptoms, ameliorates memory impairment, as well as suppresses apoptosis and enhances cell proliferation in the hippocampus of maternal-separated rat pups. *Neurosci Lett* 2011;488:26e30.
43. Okamoto K, Kurita M, Yamaguchi H, Numakura Y, Oka M (2018): Effect of tadalafil on chronic pelvic pain and prostatic inflammation in a rat model of experimental autoimmune prostatitis. *The Prostate.* 78:707–713. doi.org/10.1002/pros.23514.
44. Giuliano F, U'ckert S, Maggi M, Birder L, Kissel J and Viktrup L (2013): The Mechanism of Action of Phosphodiesterase Type 5 Inhibitors in the Treatment of Lower Urinary Tract Symptoms Related to Benign Prostatic Hyperplasia. *Eur Urol.* Mar; 63(3): 506-16. doi:10.1016/j.eururo.2012.09.006.
45. Huang S.A. and Lie J.D (2013): Phosphodiesterase-5 (PDE5) Inhibitors In the Management of Erectile Dysfunction. *P&T.* Jul; 38(7): 407, 414-419.
46. Ardehali H, O'Rourke B.(2005): Mitochondrial K(ATP) channels in cell survival and death. *J Mol Cell Cardiol* 2005;39:7:16. doi.org/10.1016/j.yjmcc.2004.12.003.
47. Mostafa T, Rashed LA and Kotb K (2010): Testosterone and chronic sildenafil/tadalafil anti-apoptotic role in aged diabetic rats T. *International Journal of Impotence Research* (2010) 22, 255–261. Doi: 10.1038/ijir.2010.12
48. Lee KW, Jeong JY, Lim BJ, Chang YK, Lee SJ, Na KR *et al.* Sildenafil attenuates renal injury in an experimental model of rat cisplatin-induced nephrotoxicity. *Toxicology* 2009; 257: 137–143.

-
49. Koupparis AJ, Jeremy JY, MuzaVar S, Persad R, Shukla N (2005): Sildenafil inhibits the formation of superoxide and the expression of gp47 NAD[P]H oxidase induced by the thromboxane A2 mimetic, U46619, in corpus cavernosal smooth muscle cells. *BJU Int* 96:423–427. doi: 10.1111/j.1464-410X.2005.05643.x.
 50. Toward TJ, Smith N, Broadley KJ (2004) Effect of phosphodiesterase-5 inhibitor, sildenafil (Viagra), in animal models of airways disease. *Am J Respir Crit Care Med* 169:227–234. doi: 10.1164/rccm.200211-1372OC.
 51. Ahluwalia A, Foster P, Scotland RS, *et al.* Antiinflammatory activity of soluble guanylate cyclase: cGMP-dependent down-regulation of P-selectin expression and leukocyte recruitment. *Proc Natl Acad Sci USA*. 2004;101:1386–1391.
 52. Vignozzi L, Gacci M, Cellai I, *et al.* PDE5 inhibitors blunt inflammation in human BPH: a potential mechanism of action for PDE5 inhibitors in LUTS. *Prostate*. 2013;73:1391–1402.23.
 53. Roumeguère T, Zouaoui Boudjeltia K, Babar S, *et al.* Effects of phosphodiesterase inhibitors on the inflammatory response of endothelial cells stimulated by myeloperoxidase-modified low-density lipoprotein or tumor necrosis factor alpha. *Eur Urol*. 2010;57:522–528.
 54. Goldsmith K, Goradia E, McClain SA, Sandoval S, Singer AJ (2020): The effect of tadalafil on reepithelialization and scarring of partial thickness porcine burns. *Wound Rep Reg*. 28:26–32. DOI:10.1111/wrr.1277
 55. Mutlu L, Arslan RS, Şahin ST, Kaya Y, Coşkun Tand Kara E (2020): The Effect of Tadalafil on Anastomotic Healing in Rats, Which Have a Small Intestinal Ischemia Reperfusion. *Asian Journal of Research in Surgery*. 4(2): 21-29.
 56. DuToit EF, Rossouw E, Salie R, Opie LH, Löhner A. Effect of Sildenafil on Reperfusion Function, Infarct Size, and Cyclic Nucleotide Levels in The Isolated Rat Heart Model. *Cardio vasc Drugs Ther*. 2005; 19:23-31.
 57. Hoke NN, Salloum FN, Kass DA, Das B, Kukreja RC (2012): Preconditioning by Phosphodiesterase-5 Inhibition Improves Therapeutic Efficacy of Adipose-Derived Stem Cells Following Myocardial Infarction in Mice. *Stem Cells*. 30:326–335. doi: 10.1002/stem.789
 58. Yardimci S, Bostanci EB, Ozer L, Dalgic T, Surmelioglu A, Aydog G, and Akoglu M (2012): Sildenafil Accelerates Liver Regeneration after Partial Hepatectomy in Rats. *Transplantation Proceedings*, 44, 1747–1750.
 59. Kim HY, Chun SY, Lee EH, Kim B, Ha Y-S, Chung J-W, Lee JN, Kim BS, Oh SH and Kwon TG (2020): Bladder Regeneration Using a Polycaprolactone Scaffold with a Gradient Structure and Growth Factors in a Partially Cystectomized Rat Model. *J Korean Med Sci*. Oct 26; 35(41): e374. doi: 10.3346/jkms.2020.35.e374.
-

الملخص العربي

تأثير تادالافيل على الموت المبرمج وانتشار الخلايا على الغشاء المخاطي المبطن للمثانة البولية بعد الالتهاب النزفي المستحث كيميائياً؛ دراسة هستولوجية وهستوكيميائية مناعية

شيرين شوقي العبد، مروة عوض عبد الحميد إبراهيم، منى تيسير صادق

قسم الهستولوجيا وبيولوجيا الخلية - كلية الطب - جامعة طنطا

مقدمة البحث: يتم استحداث التهاب المثانة النزفي كيميائياً عن طريق حقن سيكلوفوسفاميد، حيث أنه يستخدم بشكل أساسي كدواء مثبط للمناعة ومضاد للأورام. يمتلك تادالافيل المثبط للنوع الخامس من إنزيم الفوسفودايستريز خواص مضاده للالتهاب ومضادة للموت المبرمج للخلايا بجانب كونه موسع للأوعية الدموية. كما أنه من الشائع استخدامه في علاج ضعف الانتصاب وارتفاع ضغط الدم الشرياني الرئوي.

الهدف من البحث: يهدف هذا البحث إلى التحقق من تأثير تادالافيل على الموت المبرمج وانتشار الخلايا في غشاء المثانة المبطن المتضرر نتيجة الالتهاب النزفي المستحث كيميائياً.

مواد و طرق البحث: تم تقسيم ستة وثلاثين من ذكور الجرذان البيضاء عشوائياً على أربعة مجموعات. المجموعة الأولى كانت المجموعة الطابطة، عولجت المجموعة الثانية بتادالافيل، وعولجت المجموعة الثالثة بالسيكلوفوسفاميد أما الرابعة فقد عولجت بتادالافيل والسيكلوفوسفاميد معاً. تم تقسيم المجموعة الثالثة والرابعة بالتساوي إلى مجموعتين فرعيتين (a و b)، المجموعتين الفرعيتين IIIa و IVa تم التضحية بهما بعد يوم واحد، بينما تم التضحية بالمجموعتين الفرعيتين IIIb و IVb بعد عشرة أيام. تم معالجة عينات المثانة البولية للفحص المجهرى الضوئي والإلكتروني والتحليل الهستوكيميائي المناعي لل $ki67$ و caspase-3 متبوعاً بقياسات مورفومترية مختلفة.

نتائج البحث: أظهرت المجموعة الفرعية IIIa نزيف و نقص في سُمك الظهارة البولية مع وجود تقرحات تعرية للنسيج الطلائي. أظهرت المجموعة الفرعية IIIb إستعادة للظهارة البولية مع وجود مناطق محددة بها تعرية للنسيج الطلائي. كلتا المجموعتان الفرعيتان أظهرتا زيادة ذات دلالة إحصائية في الموت المبرمج للخلايا بينما أظهرت المجموعة الفرعية IIIb زيادة ذات دلالة إحصائية في انتشار الخلايا. أظهرت المجموعة الفرعية IVa نقصاً ذا دلالة إحصائية في الموت المبرمج وزيادة ذات دلالة إحصائية في انتشار الخلايا مما أدى الى الحد من فقد الخلايا. أظهرت المجموعة الفرعية IVb نقصاً ذا دلالة إحصائية في كل من الموت المبرمج وانتشار الخلايا مما يشير الى الحد من التضخم الحادث في الظهارة البولية. وقد تم التعبير عن التمايز النهائي في الخلايا السطحية للمجموعة الرابعة بوجود الخط الكفافي الزاوي وذلك عن طريق الميكروسكوب الإلكتروني النافذ.

الإستنتاج: أظهرت النتائج أن العلاج المتزامن لتادالافيل مع السيكلوفوسفاميد له تأثير إيجابي على موت الخلايا المبرمج وانتشارها وأيضاً على التغيرات الهستولوجية نتيجة التهاب الظهارة البولية النزفي. لذلك هناك حاجة الى المزيد من الدراسات لتوضيح الدور الوقائي لتادالافيل على الالتهاب النزفي المستحث بالسيكلوفوسفاميد.